J. Bangladesh Acad. Sci. 48(1); 27-34: June 2024 DOI:https://doi.org/10.3329/jbas.v48i1.68708

Journal of Bangladesh Academy of Sciences

Journal homepage: http://www.bas.org.bd/publications/jbas.html

Research Article

Effect of *p*-type doped buffer layer on the structural and magnetic properties of (Zn, Fe)Te dilute magnetic semiconductor

Indrajit Saha* and Shinji Kuroda[1]

Department of Physical and Mathematical Sciences, Chottogram Veterinary and Animal Sciences University, Khulshi, Chottogram, Bangladesh

ARTICLE INFO

Article History

Received: 10 September 2023
Revised: 19 November 2023
Accepted: 27 December 2023

Keywords: Molecular beam epitaxy, Tellurites, Magnetic materials, van-Vleck paramagnetism, Ordinary paramagnetism, Zinc-blende.

.

ABSTRACT

We have studied the structural and magnetic properties of $Zn_{1-x}Fe_xTe$ thin films grown under Te-rich flux conditions with almost the same Fe composition, x =1.3%, on both undoped and nitrogen (N) acceptor doped ZnTe buffer layer by molecular beam epitaxy (MBE). Structural analysis by XRD and XAFS reveals that $Zn_{0.987}Fe_{0.013}Te$ films have a pure diluted phase of Zinc-blende structure having Fe atoms in the substitutional position on the Zn-site in both cases. However, the magnetization measurement using SQUID shows distinctly different *M-H* curves for these films; the linear nature of magnetization on magnetic field (*M-H*), namely, van-Vleck paramagnetic behavior of $Zn_{0.987}Fe_{0.013}Te$ film grown over undoped ZnTe turns into ordinary paramagnetic behavior with S-shape *M-H* curve for film grown on N-doped ZnTe buffer layer, [N] $\approx 10^{20}$ cm^{-3} which may reflect the impact of interfacial holes provided by N-acceptors on the valence state of substitutional Fe.

Introduction

Diluted Magnetic Semiconductors (DMSs) comprise a group of semiconductor materials in which a considerable amount of host atoms are substituted by transition metals or rare earths (lanthanides) having incomplete 3d or 4f shells, respectively. Among most of the studied DMSs, the impurity band developed from these open d or f shells has been observed to be located in the mid-gap region of the host material and, hence, supplies only the magnetic moment but no extra carriers (Dietl, 1981; Vonsovskii, 1974; Sato and Katayama-Yoshida, 2002). (Zn, Fe) Te belongs to the same category of DMS with $Fe^{2+/3+}$ impurity level residing at 150 me Vin the band gap region of ZnTe, as confirmed by experimental observations (Jantsch and Hendorfer, 1990; Szadkowski, 1990). First-principle calculations for substitutional Fe on the Zn-site of the ZnTe matrix have evidenced that the interaction between the Fe ions is antiferromagnetic in nature and the stable magnetic state of (Zn,Fe)Te is paramagnetic (Sato and Katayama-Yoshida, 2002). This theoretical observation has later been experimentally verified for both bulk crystals and epitaxial layers grown by MBE (Twardowski, 1990; Malguth et al., 2008; Ishitsuka et al., 2014; Nakamura et al., 2017). The magnetization results have confirmed van-Vleck paramagnetic behavior as the intrinsic magnetic properties of (Zn, Fe)Te with very low Fe composition (Fe ≈1.6%) (Twardowski, 1990). Accordingly, $Zn_{1-x}Fe_xTe$ thin films maintain the pure dilute zinc-blende (ZB) phase of ZnTe and exhibit van-Vleck type paramagnetic behavior for Fe composition, $x \leq 0.02$ (Ishitsuka et al., 2014; Nakamura et al., 2017).

However, for such DMSs, engineering the Fermi level position with additional charge co-doping or

*Corresponding author:<indrajits.cvasu@gmail.com>

[1]*Institute of Materials Science, University of Tsukuba, Tennoudai, Tsukuba, Japan*

controlled deviations of stoichiometry has remained an efficient way to change the valence state of magnetic ions, and hence, modify the magnetic properties (Kuroda et al., 2007; Dietl and Ohno, 2006; Dietl et al., 2015; Dietl, 2006).We have already performed similar experimental studies on N-acceptor co-doped $Zn_{1-x}Fe_xTe$ thin films with Fe composition, $x \leq 0.02$, grown under different growth conditions (Saha et al., 2019; Saha et al., 2020). Since the position of N acceptor levels is just below the $Fe^{2+/3+}$ deep donor levels in the band gap region of ZnTe (Jantsch and Hendorfer, 1990; Szadkowski, 1990; Grun et al., 1996), the capturing of holes supplied by N acceptor can alter the valence state of isoelectronic Fe^{2+}, which has indeed been evidenced in our studies (Saha et al., 2019; Saha et al., 2020). The van-Vleck paramagnetic behavior of (Zn, Fe)Te thin films has transformed to room temperature ferromagnetic behavior in N-doped (Zn, Fe)Te films for [N] = 10^{18} cm^{-3} (Saha et al., 2020). This modification of magnetic properties has been explained based on the deviation of the Fe valence state from isoelectronic Fe^{2+} to $Fe^{2+/3+}$ mixed states due to N-doping. As a result, Fe ions can produce finite magnetic moments even without applying an external magnetic field and hence, the exchange interaction among the magnetic ions may change (Saha et al., 2020). We have also verified the impact of stoichiometry deviation on the magnetic properties of (Zn, Fe)Te thin films experimentally by varying the Te/Zn flux ratios during the growth (Saha et al., 2022).

DMSs that have ferromagnetic properties above room temperature are of great interest to spintronics applications (Ohno, 1998). Since future spintronics devices are expected to be composite heterostructures, the growth of (Zn, Fe)Te on *n*- or *p*-type doped buffer layer is necessary for any spin injection devices. The magnetic and transport properties of $Ga_{1-x}Mn_xAs$ thin films grown on Be (*p*-type) doped GaAs buffer layer have shown significant differences from those grown on an undoped GaAs buffer layer (Yoon et al., 2004). The magnetic properties of $Ga_{1-x}Mn_xAs$ thin film have been significantly improved by using *p*-type doped buffer layer. However, the magnetic properties of $Zn_{1-x}Fe_xTe$ thin films grown on either *n*- or *p*-type buffer layer have yet to be studied. The ionization energy of N in ZnTe has been measured at 53.4 ±1 meV, which decreases rapidly with the increase of the doping level (Baron et al., 1998). For ZnTe, by bringing the radio frequency (rf) or direct current (DC) glow plasma source closer to the substrate, hole density up to 10^{20} cm^{-3} can be achieved for N-doping concentrations, [N] ≈ 1.5 × 10^{20} cm^{-3} (Baron et al., 1998; Han et al., 1993; Baron et al., 1995). At this doping level, ZnTe shows metallic behavior with resistivity down to $\rho \approx 5 \times 10^{-3}\Omega$ cm and mobility, $\mu_h \approx 10$ cm^2/ Vs at 10 K (Baron et al., 1998). These exciting properties of the heavily N-doped ZnTe layer, together with the remarkable enhancement of magnetic properties of (Zn, Fe)Te due to N-acceptor (*p*-type) co-doping (Saha et al., 2019; Saha et al., 2020), has inspired us to investigate the impact of interfacial holes on the structural and magnetic properties of $Zn_{1-x}Fe_xTe$ thin films grown on N-acceptor doped ZnTe buffer layer which are expected to be different from those grown on undoped ZnTe buffer layer.

Materials and Methods

$Zn_{1-x}Fe_xTe$ thin films are grown with Fe composition almost fixed at $x \approx 0.013$ in ultra-high vacuum condition of 10^{-10} Torr inside a molecular beam epitaxy (MBE) chamber having Zn, Te and Fe elemental solid sources. Films are grown on GaAs (001) substrate. In the case of conventional sample (#1) ($Zn_{0.987}Fe_{0.013}Te$ on ZnTe), a thick buffer layer of ZnTe (~600 nm) is grown before the growth of $Zn_{0.987}Fe_{0.013}Te$ layer (~40 nm) to relax the large lattice mismatch. However, in the case of modulation doped sample (#2) ($Zn_{0.987}Fe_{0.013}Te$ on *p*-type ZnTe), The N-doped ZnTe layer (~300 nm) is additionally grown in between the ZnTe (~600 nm) and $Zn_{0.987}Fe_{0.013}Te$ (~40 nm) layer. During the growth of the ZnTe: N layer, radio frequency (rf) plasma has been employed to excite a nitrogen plasma source filled with N_2 gas at 300 W and a flow rate of 0.3

cm^3/min. We have kept the shutter of the plasma source positioned at 2 cm from the substrate fully open during the growth of the N-doped layer. In both cases, we deposited a thin ZnTe cap layer (~2 nm) on the magnetic layer to avoid surface oxidation during air exposure. All epitaxial layers are grown at substrate temperature of 260°C except the cap layer, which is grown at low temperature. The Beam Equivalent Pressures (BEPs) of Zn and Te during the growth of both the buffer layer and magnetic layer have been kept at 2.0×10^{-7} and 4.6×10^{-7} Torr respectively, to achieve Te-rich growth mode (Te/Zn flux ratio ≈ 2.3) for films (#1) and (#2). The BEPs are measured both before and after the growth of each epitaxial layer with the help of an ion gauge by placing it at the growth position.The flux of the effusion cells depends on the cell temperature measured by the thermocouple placed in contact with the cell crucible. Reflection high energy electron diffraction (RHEED) has been used to monitor the in-situ of the film surface during growth. The (2 × 1) streak pattern is maintained throughout $Zn_{0.987}Fe_{0.013}Te$ film (#1) growth over the ZnTe buffer layer. However, in the case of the film (#2), the (2×1) RHEED pattern changes from streak to spotty after the growth of the N-doped ZnTe layer. A similar type of spotty pattern has been observed for $Zn_{1-x}Fe_xTe$: N films with [N] > 10^{19} cm^{-3} (Saha et al., 2019; Saha et al., 2020). The Fe concentration of the films was measured by using an electron probe microanalyzer (EPMA). X-ray diffraction (XRD) θ-2θ scan has been utilized to accomplish the structural characterizations of the grown films to identify any possible precipitates of secondary phases. X-ray absorption fine structure (XAFS) measurements have been performed at the beamline BL12C of KEK-PF to investigate the surrounding environment of Fe in the films. Since the concentration of the material of interest is very low, the fluorescence-detection mode has been chosen for the Fe K-edge XAFS spectrum and measured at a low temperature of around 20 K. A Si (111) double crystal monochromator has been used to adjust the intensity of the incident X-ray monochromatic beam, and a nitrogen-filled ionization chamber has been employed for monitoring. An array of 19 Ge detector elements helps to detect the fluorescence signal. The magnetization measurements were accomplished with the help of a superconducting quantum interference device (SQUID) magnetometer with magnetic field applied normal to the film plane. The dependences of magnetization on magnetic field (*M-H*) and on temperature (*M-T*) have been performed to explain different aspects of the magnetic properties (Kuroda et al., 2007).

Results and Discussion

First, the result of XRD θ-2θ scan profiles has been discussed to analyze the structural properties of $Zn_{0.987}Fe_{0.013}Te$ films grown over undoped (#1) and N-doped (#2) ZnTe buffer layer as shown in Fig.1. In both cases, diffraction peaks only from the ZnTe buffer layer and GaAs substrate have been detected. However, for the film (#2) [$Zn_{0.987}Fe_{0.013}Te$/ZnTe: N], Peaks from the ZnTe and ZnTe: N layer have appeared separately for the (400) and (600) diffractions. A similar type of lattice parameter difference between the undoped and doped layer of ZnTe has been observed in the XRD pattern of ZnTe: N/ZnTe pseudosuperlattices for N concentrations, [N] ≈ 10^{19} cm^{-3} (Baron et al., 1998). The introduction of nitrogen atoms into the ZnTe crystal in the N_{Te} configuration with [N_{Te}] = 10^{19} cm^{-3} can produce a relative change of -1.3×10^{-4} in the lattice parameter (Baron et al., 1998). This change in lattice parameter has been estimated based on the change in ionic radii, δd ≈ -0.062 nm, when one N atom (r_N = 0.07 nm) replaces one Te atom (r_{Te} = 0.132 nm). As we have deposited heavily N-doped ZnTe layer above the undoped ZnTe layer for $Zn_{0.987}Fe_{0.013}Te$ film [#2], separated diffraction peaks from the ZnTe layer and ZnTe: N layer for the (400) and (600) diffractions are expected. From this deviation of lattice constant, *a*, the concentration of nitrogen atoms in the substitutional site on Te-site has been measured as [N_{Te}] = 2.7×10^{20} cm^{-3} following the linear relationship between *a* and [N_{Te}] reported (Baron et al., 1998). Thus, the overall XRD results have confirmed that both films (# 1) and (# 2) have

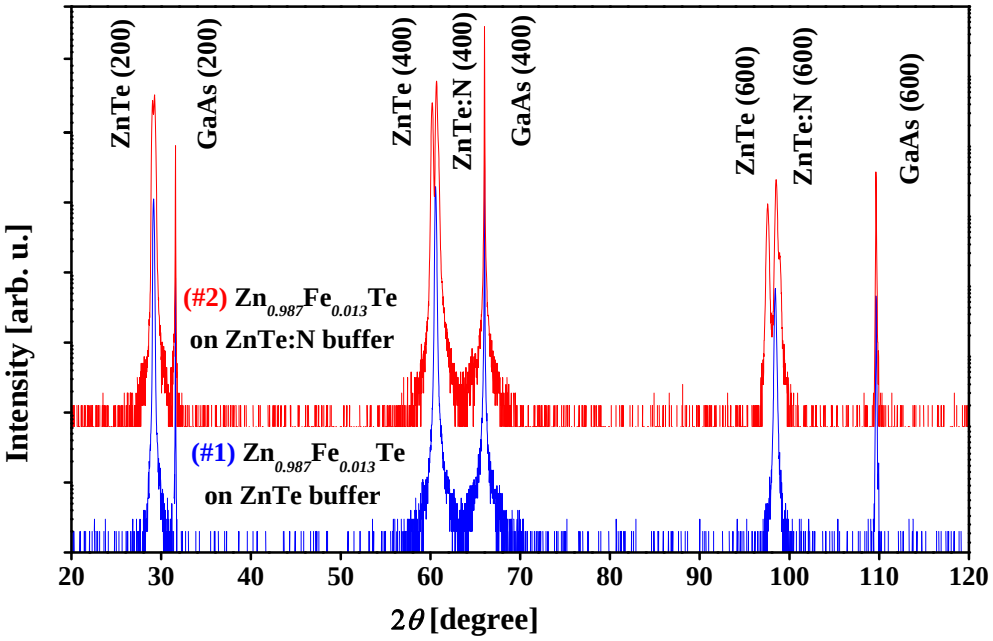

Fig. 1 The XRD θ-2θ scan profiles of $Zn_{0.987}Fe_{0.013}Te$ thin films (# 1) and (# 2) of thickness ≈ 40 nm grown over the un-doped and N-doped ZnTe buffer layer respectively.

pure diluted ZB phase of ZnTe with substitutional Fe atoms staying on the Zn site.

To examine the surrounding environment of Fe on the atomic dimension, XAFS measurements have been carried out for Fe K-edge in Zn $_{0.987}$Fe$_{0.013}$Te thin films. Since the Fe concentration (1.3%) is very low in our sample, we have to choose the fluorescence-detection mode, which is very effective for low-concentrated elements of interest (Koningsberger and Prins, 1998). In this detection mode, thick samples are generally used to achieve better signal-to-noise levels. Fig. 2 represents the result of XAFS measurement of Zn $_{0.987}$Fe$_{0.013}$Te films (#1) and (#2) of thickness ≈ 700nm, which clarifies the fact that Fe atoms incorporatesubstitutionally on the Zn site in ZnTe crystal for such as Fe concentration. The Fourier transforms of extended X-ray absorption fine structure (EXAFS) oscillation have been used to explain the experimental radial distribution function (RDF) curves around the Fe atom, which closely resemble the result of simulation for the substitutional Fe on the Zn-site in the zinc-blende (ZB) structure as shown in Fig. 2(a). The main peak at around 2.5 Å describes the bond length of Fe with Te atoms as the first nearest neighbor (1st NN). In plotting the RDF spectra, we have weighted the oscillatory parts $\chi(k)$ of EXAFS at Fe K-edge by k^3 and transformed them into real space. In the simulation curve, the substitutional Fe on the Zn-site is assumed to produce no change in the lattice constant of the ZnTe crystal and the single scattering path has been chosen.

The X-ray absorption near edge structure (XANES) spectra of the films have been demonstrated in Fig. 2(b), along with the spectrum of an elemental Fe foil. The XANES spectra of Zn $_{0.987}$Fe$_{0.013}$Te films are very different from that of elemental Fe foil, showing three absorption peaks near the Fe K-edge: the pre-edge peak at 7.1096 keV, the shoulder peak at 7.1165 keV and the main peak at 7.1238 keV. The pre-edge peak corresponds to the transitions from the 1s state to the 3d-like state (quadrupolar), while both

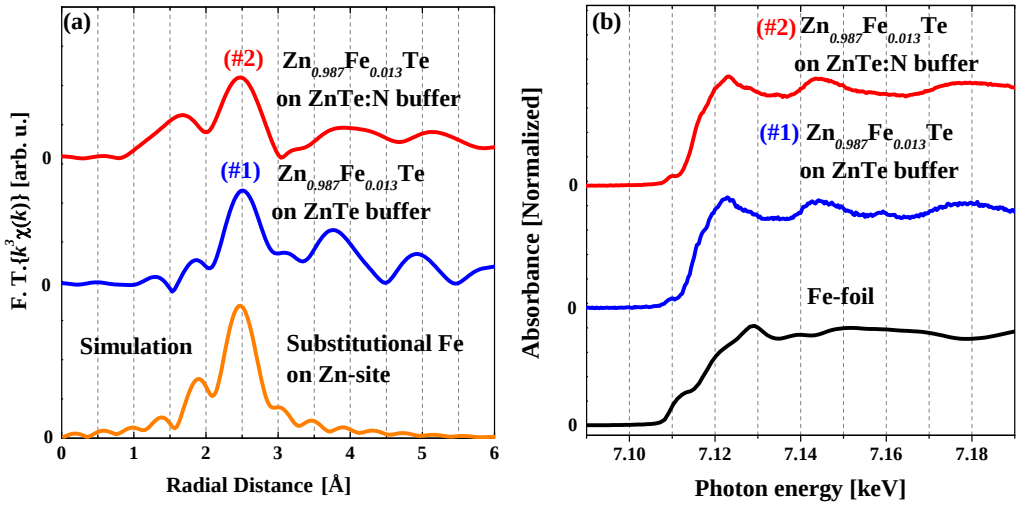

Fig. 2 shows the (a) RDF and (b) XANES spectra of $Zn_{0.987}Fe_{0.013}Te$ (# 1) and (# 2) thin films (thickness ≈ 700 nm) grown on un-doped and N-doped ZnTe respectively. Experimental RDF and XANES spectra are compared by simulating an substitutional Fe atom on the Zn-site in the ZB structure and spectra for an elemental Fe foil as shown in Fig. 2(a) and (b) respectively.

the shoulder and main peaks explain the transition from the 1s state to the 4p-like state (dipolar) (Westre et al., 1997). Through these observed RDF and XANES spectra of Zn $_{0.987}$Fe$_{0.013}$Te films, we have confirmed the pure diluted ZB phase of ZnTe has been maintained with Fe atoms incorporated in the substitutional site on the Zn-site.

The magnetization measurements have been carried out in a SQUID magnetometer by applying external magnetic field normal to the film plane. Fig. 3 (a) shows *M-H* curves for Zn $_{0.987}$Fe$_{0.013}$Te films (#1) and (#2) grown on undoped and N-doped ZnTe respectively, at 2 K. Fig. 3 (b) shows *the M-H* curve of the film (#2) at 300 K. The magnetization results of films (#1) and (#2) are significantly different [Fig. 3(a)]. For Zn $_{0.987}$Fe$_{0.013}$Te film (#1) grown on undoped ZnTe buffer, the magnetization increases almost linearly with the external applied magnetic field without being saturated. The linear dependence of magnetization on a magnetic field signifies the characteristics of van-Vleck paramagnetism (Twardowski, 1990); the quenching form of thelocalized magnetic moment can be energized through induction by applying an external magnetic field. On the other hand, Zn $_{0.987}$Fe$_{0.013}$Te film (#2) grown on N-doped ZnTe buffer shows ordinary paramagnetic behavior with an S-shape *M-H* curve. Since ZnTe: N layer with N-doping concentrations, [N] ≈ 10^{20} cm^{-3} can have hole density as high as 10^{20} cm^{-3} and exhibit metallic behavior (Baron et al., 1998), the growth of $Zn_{0.987}Fe_{0.013}Te$ film (#2) over heavily N-doped ZnTe buffer layer can allow delocalized holes to transfer from the buffer layer to the top of the magnetic layer. This increase in hole concentration in the magnetic layer may have deviated the valence state of substitutional Fe from isoelectronic Fe^{2+} can produce finite magnetic moments that persist even at zero external magnetic fields. Thus, we observe the ordinary paramagnetic behavior with an S-shape *M-H* curve in Zn $_{0.987}$Fe$_{0.013}$Te film (#2) grown on p-type ZnTe buffer layer instead of the conventional linear *M-H* curve of van-Vleck paramagnetism for the film (#1) grown over undoped ZnTe buffer layer. A similar type of enhancement in the magnetic properties has also been observed for GaMnAs ferromagnetic semiconductors when grown on *p*- type doped buffer layer (Yoon et al., 2004). In addition, we have already observed the Fe valence state deviation in

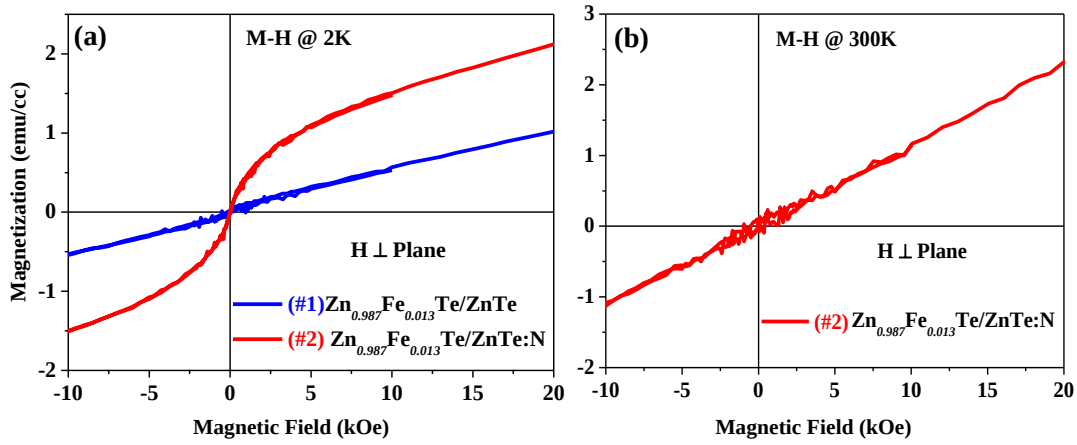

Fig. 3 (a) *M-H* curves of $Zn_{0.987}Fe_{0.013}Te$ thin films of thickness ≈ 40 nm grown over undoped (#1) and N-doped (#2) ZnTe buffer layer measured at 2 K. (b) *M-H* curve of $Zn_{0.987}Fe_{0.013}Te$ film (#2) at 300 K. Measurements are performed with magnetic field normal to the film plane.

$Zn_{1-x}Fe_xTe$ due to nitrogen acceptor co-doping and, hence, the modification of its magnetism (Saha et al., 2019; Saha et al., 2020). Thus, this finding provides evidence to modify the magnetism of $Zn_{0.987}Fe_{0.013}Te$ films indirectly (impact of interfacial holes from the *p*-type buffer). However, film (#2) has shown van-Vleck paramagnetic behavior at 300 K [Fig. 3(b)].

We have also demonstrated *M-T* curves for $Zn_{0.986}Fe_{0.014}Te$ films (#1) and (#2) grown on undoped and N-doped ZnTe buffer layers, respectively with the application of external magnetic field of 500 Oe as shown in Fig. 4. For film (#1) the cusp-like magnetic behavior termed as blocking phenomenon has beenobserved in the zero-field-cooled (ZFC) curve at low temperature of around 5 K [Fig. 4(a)], while both the field-cooled (FC) and zero-field-cooled (ZFC) curves show monotonic increase with lowering temperature without such blocking phenomena in film (#2) [Fig. 4(b)].

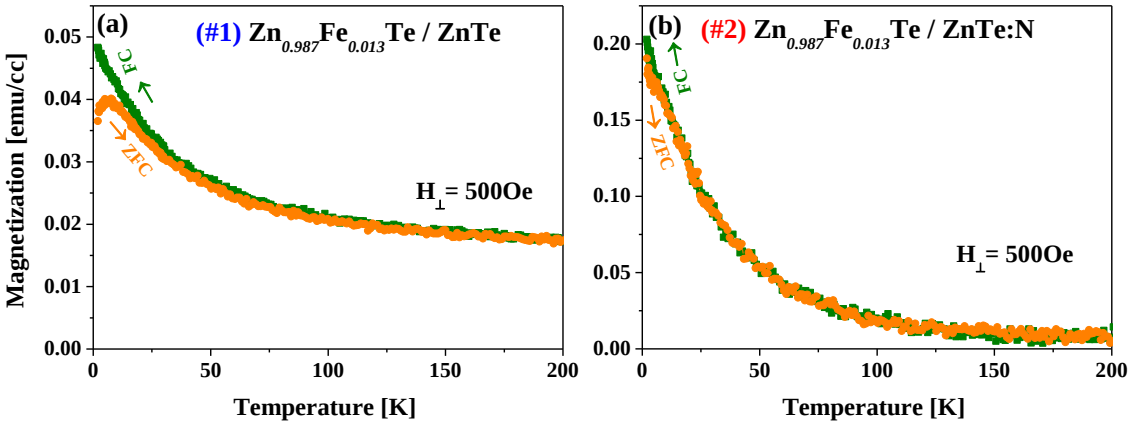

Fig. 4 *M-T* curves of $Zn_{0.987}Fe_{0.013}Te$ thin films of thickness ≈ 40 nm grown over (a) undoped (#1) and (b) N-doped (#2) ZnTe buffer layer. Field-cooled (FC) and zero-field-cooled (ZFC) magnetization have been measured by applying 500 Oe constant magnetic field normal to the film plane.

The blocking phenomenon, a feature of superparamagnetism, is usually seen in magnetically inhomogeneous systems (Dietl et al., 2015; Sato et al., 2007; Devillers et al., 2007). In such a system, the clustering of local regions may exhibit ferromagnetism inside the crystal; at low temperatures, the magnetic anisotropy can effectively inactivate the magnetic moments of these regions and suppress the resulting magnetization. Based on the result of the XAFS measurement, we can exclude the possibility of the formation of precipitates, so the clustering of substitutional Fe on the Zn-site in ZnTe may be the source of the blocking phenomenon. However, the FC and ZFC magnetization values at low-temperature regions are largely different in the *M-T* curves of these films (#1) and (#2); higher values of magnetization are observed in film (#2) grown on N-doped ZnTe buffer layer. Similar FC and ZFC magnetization tendencies have also been noticed in (Zn, Fe)Te: N thin films compared to undoped (Zn, Fe)Te thin films. (Saha et al., 2019; Saha et al., 2020).

Conclusion

We have investigated the structural and magnetic properties of $Zn_{0.987}$ $Fe_{0.013}Te$ thin films grown on undoped and N-doped ZnTe buffer layer by MBE. XRD and XAFS have ensured the zinc-blende crystal structure of the films with Fe atoms substituting the Zn-site. However, SQUID measurements reveal different magnetic behavior among these films; van-Vleck paramagnetic behavior (linear *M-H* curve) of the film grown on undoped ZnTe buffer transforms to S-shape *M-H* curve of ordinary paramagnetic behavior for the film grown over N-doped ZnTe buffer layer. This enhancement in the magnetic properties may happen; Since the heavily N-doped ZnTe layer, [N] $\approx$ 10^{20} cm^{-3}, can accommodate as high as 10^{20} cm^{-3} delocalized holes at the interface with the (Zn, Fe)Te layer, the trapping of holes by the Fe 3*d* levels alter the isoelectronic Fe^{2+} ions valence state. This deviation of valence state can introduce finite magnetic moment in (Zn, Fe)Te even without an external magnetic field. Thus, these experimental findings have opened the scope of future research studies of controlling the magnetic properties of (Zn, Fe)Te by external means, such as by applying electric field or irradiation of light, which may impact substitutional Fe ions valence state and the resultant magnetic properties of (Zn,Fe)Te.

Acknowledgment

The collaboration between the Semiconductor Spintronics laboratory, Institute of Materials Science, University of Tsukuba, Japan, and the High Energy Accelerator Research Organization (KEK), Tsukuba, Japan, is greatly acknowledged.

References

Baron T, Saminadayar K and Magnea M. Nitrogen doping of Te-based II-VI compounds during growth by molecular beam epitaxy. *J. Appl. Phys.*1998; 83: 1354-1370.

Baron T, Saminadayar K and Magnea M. Nitrogen doping of tellurium-based II-VI compounds during growth by molecular beam epitaxy. *Appl. Phys. Lett.* 1995; 67: 2972-2974.

Devillers T, Jamet M, Barski A, Poydenot V, Bayle-Guillemaud P, Belet-Amalric E, Cherifi S and Cibert J. Structure and magnetism of self-organized $Ge_{1-x}Mn_x$ nanocolumns on Ge(001). *Phys. Rev. B* 2007; 76: 205306.

Dietl T, Sato K, Fukushima T, Bonanni A, Jamet M, Barki A, Kuroda S, Tanaka M, Hai PN and Katayama-Yoshida H. Spinodal nanodecomposition in semiconductors doped with transition metals. *Rev. Mod. Phys.* 2015; 87: 1311-1377.

Dietl T and Ohno H. Engineering magnetism in semiconductors. *Materi. Today* 2006; 9: 18-26.

Dietl T. Self-organized growth controlled by charge states of magnetic impurities. *Nat. Mater.* 2006; 5: 673.

Dietl T. Semimagnetic semiconductors in magnetic fields. Chikazumi S. and Miura N. (Eds.), In: *Physics in High Magnetic Fields*. Springer, Berlin; 1981, pp. 344-354.

Grun M, Haury A, Cibert J and Wasiela A. The nitrogen acceptor energy in ZnTe measured by Hall effect and optical spectroscopy. *J. Appl. Phys.* 1996; 79: 7386-7388.

Han J, Stavrinides TS, Kobayashi M, Gunshor RL, Hageroot MM and Nurmikko AV. Heavy *p*-doping of ZnTe by molecular beam epitaxy using a nitrogen plasma source. *Appl. Phys. Lett.* 1993; 62: 840-842.

Ishitsuka S, Domon T, Akiyama R, Kanazawa K, Kuroda S and Ofuchi H. Structural and magneticcharacterization of (Zn, Fe) Te thin films grown by MBE. *Phys. Stat. Sol. (C)* 2014; 11: 1312-1315.

Jantsch W and Hendorfer G. Characterization of deep levels in CdTe by photo-EPR and related techniques. *J. Cryst. Growth.* 1990; 110: 404-413.

Koningsberger DC and Prins R. *X-ray Absorption: Principles, Applications, Techniques of EXAFS, SEXAFS and XANES.* Chemical Analysis. John Wiley and Sons, New York; 1988, p. 688.

Kuroda S, Nishizawa N, Takita K, Mitome M, Bando Y, Osuch K and Dietl T. Origin and control of high-temperature ferromagnetism in semiconductors. *Nat. Mater.* 2007; 6: 440-446.

Malguth E, Hoffmann A and Philips MR. Fe in III-V and II-VI semiconductors. *Phys. Stat. Sol. (b)* 2008; 245(3): 455-480.

Nakamura T, Sugimura Y, Domon T, Ishitsuka S, Kanazawa K, Ofuchi H and Kuroda S. Structural and magnetic properties of (Zn,Fe)Te thin films grown by MBE under Zn-rich flux condition. *J. Cryst. Growth.* 2017; 477: 123-126.

Ohno H. Making nonmagnetic semiconductors ferromagnetic. *Science.*1998 ; 281 : 951-956.

Saha I, Kanazawa K, Nitani H and Kuroda S. Impact of growth conditions on the structural and magnetic properties of (Zn, Fe)Te thin films grown by molecular beam epitaxy (MBE). *J. Cryst. Growth.* 2022; 580: 126492.

Saha I, Nakamura T, Kanazawa K, Nitani H, Mitome M, and Kuroda S. Nitrogen co-doping affects the structural and magnetic properties of (Zn, Fe)Te. *J. Cryst. Growth.* 2019; 511: 42-47.

Saha I, Tomohiro Y, Kanazawa K, Nitani H and Kuroda S. Structural and magnetic properties of nitrogen acceptor co-doped (Zn, Fe)Te thin films grown in Zn-rich condition by molecular beam epitaxy (MBE). *J. Electron. Mater.* 2020; 49(10): 5739-5749.

Sato K, Fukushima T and Katayama-Yoshida H. Super-paramagnetic blocking phenomena and roon temperature ferromagnetism in wide band-gap dilute magnetic semiconductor (Ga, Mn)N. *Jpn. J. Appl. Phys.* 2007; 46: L682.

Sato K and Katayama-Yoshida H. First principles materials design for semiconductor spintronics. *Semicond. Sci. Technol.* 2002; 17: 367-376.

Szadkowski AJ. The $Fe^{2+/3+}$ donor level in CdTe. *J. Phys. Cond. Matter.* 1990; 2: 9853-9859.

Twardowski A. Magnetic properties of Fe-based diluted magnetic semiconductors. *J. Appl. Phys.* 1990; 67: 5108-5113.

Vonsovskii SV. *Magnetism.* John Wiley and Sons, New York; 1974, p. 1256.

Westre TE, Kennepohl P, DeWitt JG, Hedman B, Hodgson KO and Solomon EI. A multiplet analysis of Fe K-edge 1s→3d pre-edge features of iron complexes. *J. Am. Chem. Soc.* 1997; 119: 6297-6314.

Yoon YJ, Chung SJ, Lee HJ, Lee S, An SY, Liu X and Furdyna J K. Effect of p-type buffer layer on the properties of GaMnAs ferromagnetic semiconductors. *J. Korean Phys. Soc.* 2004; 45: S720-S723.